Nonlocal electron heat relaxation in a plasma shock at arbitrary ionization number

J. Ramírez and J. R. Sanmartín
Escuela Técnica Superior de Ingenieros Aeronáuticos, Universidad Politécnica, 28040 Madrid, Spain

R. Fernández-Feria
Escuela Técnica Superior de Ingenieros Industriales, Universidad de Sevilla, 41012 Sevilla, Spain

(Received 27 July 1992; accepted 28 January 1993)

A recently obtained nonlocal expression for the electron heat flux valid for arbitrary ionization numbers Z is used to study the structure of a plane shock wave in a fully ionized plasma. Nonlocal effects are only important in the foot of the electronic preheating region, where the electron temperature gradient is the steepest. The results are quantified as a function of a characteristic Knudsen number of that region. This work also generalizes to arbitrary values of Z previous results on plasma shock wave structure.

I. INTRODUCTION

Heat transport in a fully ionized gas is mainly carried by superthermal electrons, typically with energies of about six times the thermal energy kT_e,[1] where k is Boltzmann constant and T_e is the electron temperature. As a consequence, the classical (local) Fourier law for the electron heat flux has been found to fail, contrary to usual predictions of Kinetic theory, at temperature scale lengths, $H \equiv |\nabla \ln T_e|^{-1}$, much larger than the thermal mean free path for electron scattering λ_T, usually as large as $10^2\lambda_T$. The local expression for the electron heat flux in a plasma becomes thus inappropriate whenever moderately steep temperature gradients occur. Several nonlocal expressions have been proposed in the past to model the electron heat flux,[2] which extend the validity range down to $H \sim \lambda_T$. In this work we use a recently obtained nonlocal heat flux law valid for all ionization numbers Z,[1] to study the differences introduced by nonlocal transport, as opposed to local transport, in a well-defined, and relatively simple, problem of plasma physics: The structure of a plane shock wave in a fully ionized, homogeneous, and unmagnetized plasma. This problem is both basic and very appropriate to test the validity of the local, against the nonlocal, electron heat conduction expressions.

As we shall see, within the plasma shock wave the nonlocal electron heat flux effects are only important in the electronic preheating zone preceding the ionic shock front, where the electron temperature rises from its upstream value to almost the downstream temperature. Therefore, the present analysis will be focused on that shock region, though a description of the complete shock structure, which generalizes the local results of Jaffrin and Probstein[3] for all Z, is given in the Appendix. We shall see that nonlocal electron heat transport widens the electronic preheating region in comparison with local predictions, smoothing the electron temperature profile in the foot of that region where the gradient is the steepest; the difference between both predictions is more important as either the upstream Mach number or the ionization number increase. The temperature scale length of the region of interest is always within the validity range of the nonlocal theory [$H \gtrsim O(\lambda_T)$], so that the present problem will quantify the errors of the local heat flux as H/λ_T decreases. However, the range of values of H/λ_T in the preheating region is not so wide as one would expect: As the intensity of the shock (Mach number) increases, the temperature scale length of that region decreases from $H > 10^2\lambda_T$ (where the classical Spitzer–Härm heat flux law applies), to $H \simeq 20\lambda_T$ for very strong shocks. Nevertheless, we shall see that, even for these relatively high values of H/λ_T, the modifications introduced by the nonlocal electron heat transport are locally important at the leading edge of the shock.

II. FORMULATION OF THE PROBLEM

We consider a fully ionized plasma consisting of electrons (mass m_e, charge $-e$), and ions (mass m_i, charge Ze), and look for the solution to the steady, one-dimensional, shock wave equations with no applied external electric or magnetic fields. We also assume that the Debye length is much smaller than any collisional mean-free path in the problem,[3] so that quasineutrality applies:

$$U_e = U_i \equiv U, \quad n_e = n_i Z \equiv n, \tag{1}$$

where U is the mean (one-dimensional) velocity, n is the number density, and the subscripts e and i represent electrons and ions, respectively. With this assumption, only four conservation equations for n, U, the electron temperature T_e, and the ion temperature T_i are needed. For convenience we use the electron mass, the total momentum, the total energy, and the ion energy conservation equations:

$$m_e n U = m, \tag{2}$$

$$nU^2\left(m_e + \frac{m_i}{Z}\right) + nk\left(T_e + \frac{T_i}{Z}\right) - \frac{4}{3}(\mu_e + \mu_i)\frac{dU}{dx} = P, \tag{3}$$

$$\frac{5}{2}knU\left(T_e + \frac{T_i}{Z}\right) + \frac{1}{2}nU^3\left(m_e + \frac{m_i}{Z}\right) - \frac{4}{3}(\mu_e + \mu_i)U\frac{dU}{dx} + q_{ex} + q_{ix} = E, \tag{4}$$

 0899-8221/93/051485-06$06.00

$$\frac{3}{2}kn_iU\frac{dT_i}{dx}+\frac{dq_{ix}}{dx}+\left(n_ikT_i-\frac{4}{3}\mu_i\frac{dU}{dx}\right)\frac{dU}{dx}=E_i. \tag{5}$$

In the above equations, m, P, and E are integration constants; μ_e and μ_i are the electron and ion viscosity coefficients; q_{ex} and q_{ix} are the electronic and ionic heat fluxes in the x direction; and E_i is the energy transfer between ions and electrons. Notice that m_e can be neglected against m_i/Z in Eqs. (3) and (4) ($m_eZ/m_i\simeq 2.78\times 10^{-4}$ in a fully ionized plasma). Also, since $\mu_i/\mu_e\sim m_i/m_e\gg 1$,[4] we shall neglect, as usual, the electron viscosity terms against the ionic ones in Eqs. (3)–(5). The ionic viscosity is given by $\mu_i=\mu_0 n_i kT_i\tau_i$, where τ_i is the ion–ion collision time at thermal energies, and $\mu_0\simeq 0.96$.[4] Local expressions[4] will also be used for the ion heat flux, $q_{ix}=-\kappa_i\,dT_i/dx$, where $\kappa_i=k_0n_ikT_i\tau_i/m_i$ is the ionic thermal conductivity ($k_0\simeq 3.906$), and for E_i,

$$E_i=\frac{3m_enk}{m_i\tau_{ei}}(T_e-T_i),\quad \tau_{ei}=\frac{3m_e^{1/2}(kT_e)^{3/2}}{4(2\pi)^{1/2}e^4Z^2n_i\ln\Lambda_{ei}}, \tag{6}$$

τ_{ei} being the ion–electron collision time at thermal energies.

The main difference of the present work in relation to previous ones on plasma shock wave structure (e.g., Refs. 3 and 5), is the use of a nonlocal expression for the electron heat flux, which we take from Ref. 1:

$$q_{ex}=-\int dx'\,\frac{n'k^{3/2}T_e'^{1/2}}{4\pi(3m_eZ_*)^{1/2}}L_z^*(\theta)\frac{dT_e'}{dx'}, \tag{7}$$

where the primes denote the values of the respective variables at x', and

$$L_z^*(\theta)=8\pi^{1/2}\int_0^\infty ds\,\frac{s\exp[-s-\theta\sigma_z(s)]}{\sigma_z(s)},$$

$$\sigma_z(s)=\left(\frac{4}{3Z_*s^2}+\frac{Z_*-1}{Z_*s^3}\right)^{1/2}, \tag{8}$$

$$\theta(x,x')=\frac{\pi e^4\sqrt{6Z_*}\ln\Lambda_{ee}}{[kT_e(x')]^2}\left|\int_x^{x'}n(x'')dx''\right|,$$

$$Z_*\equiv Z\ln\Lambda_{ei}/\ln\Lambda_{ee}. \tag{9}$$

This self-consistent, nonlocal electron heat flux law is valid for all values of Z (previous nonlocal expressions were valid for $Z\gg 1$; see, e.g., Ref. 2), and reproduces the local limit for smooth enough gradients:

$$q_{ex}^l=-\frac{\gamma_0(Z)\tau_{ei}k^2T_e}{m_en}\frac{dT_e}{dx}, \tag{10}$$

$$\gamma_0(Z)\equiv\int_0^\infty d\theta\,\frac{2L_z^*(\theta)}{9\pi^{3/2}}=\frac{4Z_*}{(3\pi)}\int_0^\infty ds\,\frac{s^4e^{-s}}{[s+3(Z_*-1)/4]}, \tag{11}$$

where $\gamma_0(Z)$ ranges from $8/\pi$ for $Z=1$ to $128/(3\pi)$ for $Z\to\infty$. Expression (10) agrees quite well with exact local results (see Ref. 1). Comparing q_{ix} with (7) or (10), one finds that $q_{ix}/q_{ex}\sim\sqrt{m_e/m_i}\ll 1$, so that the ion heat flux may be omitted in (4), but should be retained in (5).

To write Eqs. (2)–(5) in dimensionless form we use the values of plasma variables far downstream ($x\to+\infty$), subsequently denoted by n_2, U_2, $T_{e2}=T_{i2}\equiv T_2$, instead of the conditions far upstream ($x\to-\infty$), n_1, U_1, T_1, because, among other reasons, the relative order of magnitude of the different terms in Eqs. (2)–(5) will not change as the upstream Mach number M_1 changes from unity to infinity (the downstream Mach number remains always order unity). Thus we define

$$\eta\equiv\frac{U}{U_2}=\frac{n_2}{n},\quad \theta_e\equiv\frac{T_e}{T_2},\quad \theta_i\equiv\frac{T_i}{T_2},\quad y\equiv\frac{x}{H}, \tag{12}$$

where H is a characteristic length appropriate for a particular region. Far upstream and far downstream all the gradients vanish in (3)–(5), and these equations reduce to the Rankine–Hugoniot relations

$$\eta_1=(M_2^2+3)/4M_2^2=4M_1^2/(M_1^2+3)>1, \tag{13}$$

$$\theta_1\equiv\theta_{e1}=\theta_{i1}=(M_2^2+3)(5M_2^2-1)/16M_2^2=16M_1^2/(M_1^2+3)(5M_1^2-1)<1,$$

$$\eta_2=1,\quad \theta_2\equiv\theta_{e2}=\theta_{i2}=1, \tag{14}$$

where

$$M_\alpha=m_iU_\alpha/[5(1+Z)kT_0/3]^{1/2},\quad \alpha=1,2, \tag{15}$$

are the upstream ($\alpha=1$) and downstream ($\alpha=2$) Mach numbers, related to each other through

$$M_2^2=(M_1^2+3)/(5M_1^2-1). \tag{16}$$

Thus when M_1 increases from 1 to ∞, M_2 decreases from 1 to $\sqrt{1/5}$, remaining always order unity.

As described by Jaffrin and Probstein[3] for the local limit, when $Z=O(1)$, Eqs. (2)–(5) have two characteristics lengths H, which give rise to three distinguished regions where different collisional effects are important. There is a first region (I or electronic preheating region) of thickness $H_{\rm I}\sim\lambda_{i2}\sqrt{m_i/m_e}$ and, therefore, much thicker than the thermal mean-free path for ion–ion scattering $\lambda_{i2}\equiv\sqrt{kT_2/m_i}\tau_{i2}$ (τ_{i2} is the thermal ion–ion collision time based on downstream conditions), where the ion energy and momentum transport are negligible, so that the only dissipative mechanisms are the (nonlocal) electron heat flux and the energy transfer between ions and electrons; in this region we shall see that the electron temperature θ_e raises from θ_1 to almost its final value $\theta_2=1$. There may next exist a second, much thinner region (II or ionic shock front) of thickness $H_{\rm II}\sim\lambda_{i2}$, where θ_e is almost constant but ion velocity and temperature are not. Finally, there is a third region (III or ion-temperature relaxation zone), of similar thickness than region I ($H_{\rm III}\sim H_{\rm I}\sim\lambda_{i2}\sqrt{m_i/m_e}$) where the ion temperature relaxes from the high value reached in II to θ_2 by ion–electron collisions. Regions I and III are described by the same simplified equations. Making $H_{\rm I}=a\lambda_{i2}\sqrt{m_i/m_e}Z^3/(1+Z)^{3/2}$, where

$a=6\sqrt{3}\gamma_0(Z)\ln\Lambda_{ii}/(5\sqrt{5}\ln\Lambda_{ei})$, and neglecting terms of order $\lambda_{i2}/H_I\sim\sqrt{m_e/m_i}\ll 1$, Eqs. (2)–(5) may be written as

$$0=\eta-1+\frac{3}{5M_2^2}\left(\frac{Z}{1+Z}\frac{\theta_e}{\eta}+\frac{1}{1+Z}\frac{\theta_i}{\eta}-1\right), \tag{17}$$

$$\left(\int_0^\infty d\theta\, L_z^*(\theta)\theta_e^{5/2}\frac{d\theta_e}{dy}\right)\Big/\int_0^\infty d\theta\, L_z^*(\theta)$$
$$=4M_2^3(\eta-1)(\eta_1-\eta), \tag{18}$$

$$\frac{d\theta_i}{d\eta}+\frac{2}{3}\frac{\theta_i}{\eta}\frac{d\eta}{dy}=\frac{\gamma_0(Z)}{M_2}\left(\frac{6}{5}\frac{Z}{1+Z}\right)^2\frac{\theta_e-\theta_i}{\eta^2\theta_e^{3/2}}. \tag{19}$$

Notice that the total momentum conservation equation becomes algebraic in these two regions, and the problem is reduced there to solving two coupled integrodifferential equations for, say, η and θ_e.

Local linear analysis near the end singular points (see Appendix) shows that for weak shocks, more precisely, for

$$M_2^2>\frac{5+3Z}{5(1+Z)}\equiv M^* \quad\text{or}\quad M_1^2<\frac{10+9Z}{5(2+Z)}, \tag{20}$$

the above equations describe the evolution of the plasma throughout the shock, so that regions I and III merge, and the much thiner region II does not exist (one has a relaxation shock,[5] where the ionic heat conduction and viscosity do not play any important role). Notice that the largest value of M_1 for which a continuous solution in the absence of viscosity is possible is given here for arbitrary values of Z [Eq. (20)]; for $Z\to\infty$ it coincides with the corresponding value for a neutral monatomic gas,[5] while for $Z=1$ it coincides with that given in Ref. 3.

For stronger shocks (i.e., $M_2^2<M^*$), Eqs. (17)–(19) yield a discontinuity somewhere inside the shock which separates regions I and III, as described above. This discontinuity constitutes the inner ionic shock (region II) when one looks at the shock equations with the scale $H_{II}\sim\lambda_{i2}$. In this scale, Eq. (4) yields, at the lowest order, $\theta_e=\text{const}\equiv\theta_3$, and Eq. (5) may be integrated once. Making $H_{II}=4\mu_0\lambda_{i2}/[15(1+Z)]^{1/2}$, Eqs. (3) and (5) in the ionic shock become

$$\frac{\theta_i^{5/2}}{M_2}\frac{d\eta}{dy}=\eta-1+\frac{3}{5M_2^2}\left(\frac{Z}{1+Z}\frac{\theta_e}{\eta}+\frac{1}{1+Z}\frac{\theta_i}{\eta}-1\right), \tag{21}$$

$$\frac{k_0}{2\mu_0}\frac{\theta_i^{5/2}}{M_2}\frac{d\theta_i}{dy}=\theta_i+\frac{5(1+Z)M_2^2}{9}\eta(\eta-2)$$
$$+\frac{2}{3}[Z\theta_3\ln\eta-(1+Z)\eta]+G, \tag{22}$$

where G is an integration constant. The end points of this inner ionic layer, (θ_{i3},η_3) and (θ_{i4},η_4), and the electronic temperature θ_3, are obtained by neglecting all the gradients in Eqs. (21) and (22), and solving the resulting algebraic equations jointly with the numerical solutions of Eqs. (17)–(19) in regions I and III (see the Appendix).

For smooth enough electron temperature gradients, the left hand side of Eq. (18) becomes $\theta^{5/2}\,d\theta/dy$, and one recovers the local shock wave equations. In the Appendix we sketch the solution of Eqs. (17)–(19), (21), and (22) in this local limit, generalizing the solution of Jaffrin and Probstein[3] (which is for $Z=1$) for any value of Z. It is shown there that θ_3 is always almost unity, the difference $1-\theta_3$ being smaller as either M_2 or Z increase (see Fig. 4 in the Appendix). Therefore, the electron temperature rises in region I from the upstream value θ_1 to almost its final value, so that the differences introduced by the nonlocal electron heat flux formulation in the shock structure will be located, if they exist at all, only in the electronic preheating region. Hence, the results given in the next section will be obtained taking into account only Eqs. (17)–(19) for that region. We shall see that the thickness of region I increases in relation to local predictions. But before presenting these results we consider the limit $Z\gg 1$, for which the shock equations are considerably simplified.

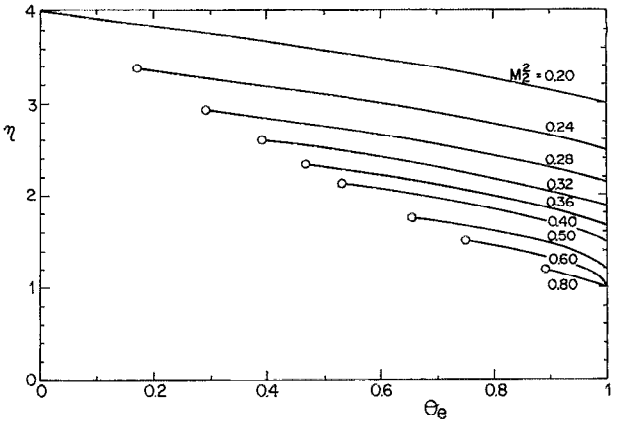

FIG. 1. Solutions in the (θ_e,η) phase plane for different Mach numbers in the limit $Z\gg 1$.

A. Limit $Z\gg 1$

In this limit one finds that the thickness of regions I and III is of order $\lambda_{i2}\sqrt{m_i/m_e}Z^{3/2}$. The equations in these zones become much simpler than Eqs. (17)–(19) because the ionic temperature is decoupled from the electronic temperature and velocity at the lowest order in Z^{-1}; from Eq. (17), one has

$$0=\eta-1+(3\theta_e/5M_2^2\eta), \tag{23}$$

which, when substituted into Eq. (18), yields an integral equation where only θ_e appears. Once θ_e and η are known, θ_i is obtained from Eq. (19) (making $Z\to\infty$). Equation (23) is an algebraic solution of the problem in (θ_e,η) phase plane. It is easily shown (see Fig. 1), that this solution is uniformly valid thoughout the shock wave for $M_2^2>3/5$ (or $M_1^2<9/5$), which is the limit $Z\gg 1$ of (20). When $M_2<3/5$, a discontinuity should appears somewhere in the shock in order for (23) to satisfy both boundary conditions, $\theta_e(\eta_1)=\theta_1$ and $\theta_e(\eta_2)=\theta_2$. This *discontinuity*, when looked at with the scale where ionic transport becomes important, constitutes, of course, the inner ionic shock. The position and intensity of this inner shock may be obtained, as in the case $Z=O(1)$ (see Appendix), from

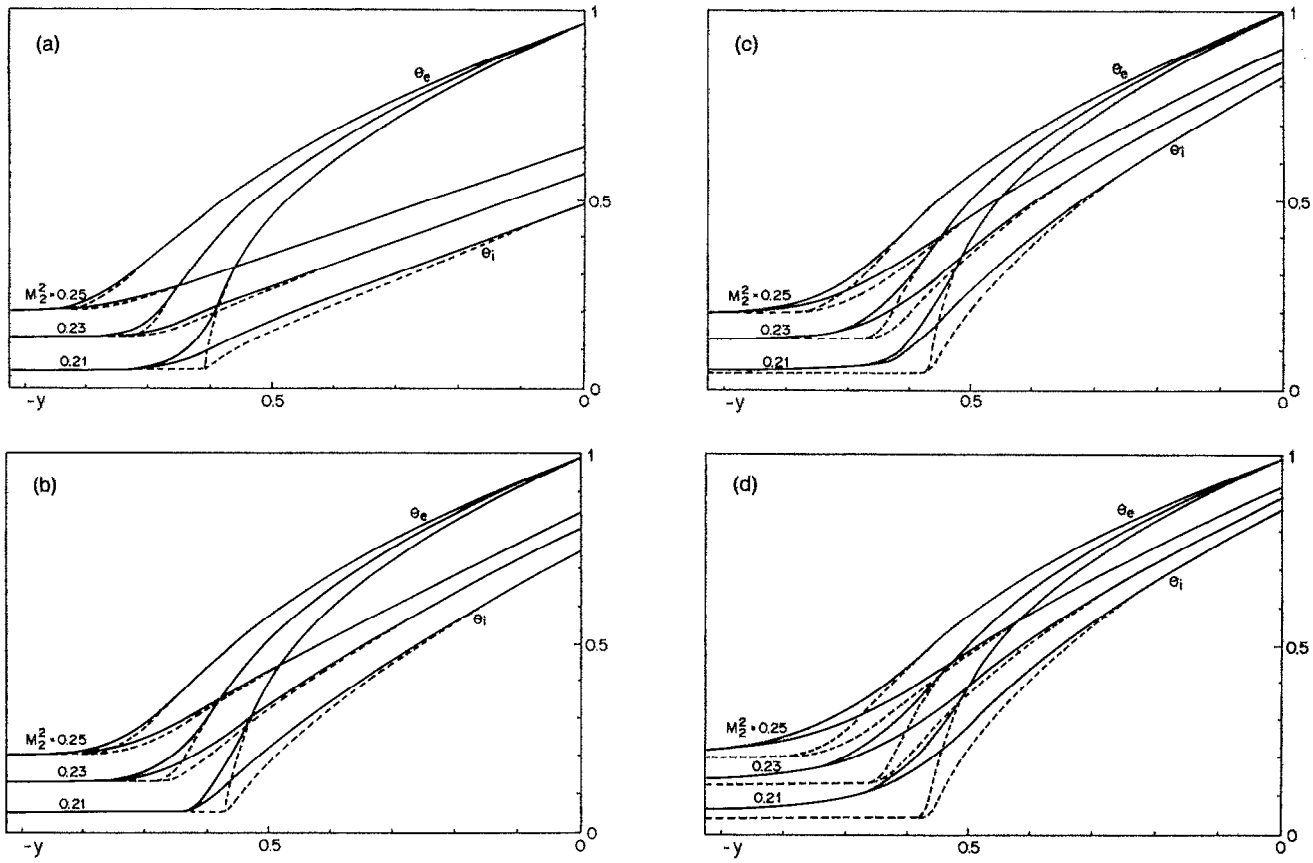

FIG. 2. Electron (θ_e) and ion (θ_i) temperature profiles with local (dashed lines) and nonlocal (continous lines) electron heat fluxes, for (a) $Z=3$, (b) $Z=10$, (c) $Z=30$, and (d) $Z=100$, and for the Mach numbers $M_1=3.6$, 4.6, and 8 ($M_2^2=0.25$, 0.23, and 0.21, respectively).

the coupling of Eqs. (17)–(19) with the equations governing the inner scale. As a difference with respect to the case $Z=O(1)$, when $Z\gg1$ the ionic temperature rises enormously in this inner ionic shock, and becomes order Z. Consequently, the thickness of the inner shock is of order $\lambda_{i2}Z^2$. Defining now $H'_{II}\equiv 4\mu_0\lambda_{i2}Z^2/\sqrt{15}$ and $\theta_i^*\equiv\theta_i/Z$, the equations governing η and θ_i^* in this inner layer are the same Eqs. (21) and (22), but neglecting 1 against Z, dropping Z, and substituting θ_i by θ_i^*. As in the case $Z=O(1)$, it is not necessary to solve these equations for the inner shock in the present study because $\theta_3\simeq1$ (more even so when $Z\gg1$, see Appendix) and the electronic heat flux is negligible in the inner shock and in the subsequent relaxation zone.

III. RESULTS AND DISCUSSION

To solve the integrodifferential Eqs. (17)–(19) [or the simpler ones (23), (18), and (19) for $Z\gg1$] in the electronic preheating region of interest we use an iterative scheme: We start with the local profiles $\theta_e(y)$, $\eta(y)$, and $\theta_i(y)$, assuming the ionic shock front as a discontinuity in the scale length H_I (see the Appendix), and substitute them into Eqs. (17)–(19) to obtain improved profiles; the procedure is repeated until the electron heat fluxes obtained by two successive iterations differ less than 0.1%. The number of iterations for the cases solved ranged from 9 for $Z=100$, $M_1=8$, to 19 for $Z=3$, $M_1=3.6$.

Figure 2 shows some electron and ion temperature profiles, $\theta_e(y)$ and $\theta_i(y)$, for different values of M_1 and Z, and compares them with the corresponding local profiles (only region I is shown because regions II and III coincide with local predictions; see Fig. 5 in the Appendix for the complete local shock structure in a particular case). The differences between local and nonlocal predictions increase as either M_1 or Z increase, and they are located in the foot of the preheating region where the local gradients are the steepest. These differences are better quantified in Fig. 3, where we plot the dimensionless thickness of the preheating region, defined as $\Delta y\equiv(\theta_2-\theta_1)/(d\theta_e/dy)_{max}$, for the same cases of Fig. 2, and for both the local and the nonlocal formulations. It is observed that Δy depends, mostly, on the Mach number, and that for high M_1 and Z (e.g., for $M_1=8$ and $Z=100$), the nonlocal value of Δy may be even three times larger than the local one.

To check the validity of the above results it is interesting to compute the *Knudsen number*, ratio λ_T/H between the mean-free path for scattering of thermal electrons and the characteristic length of region I, as a function of M_1 and Z. The characteristic length of the electronic preheating region is

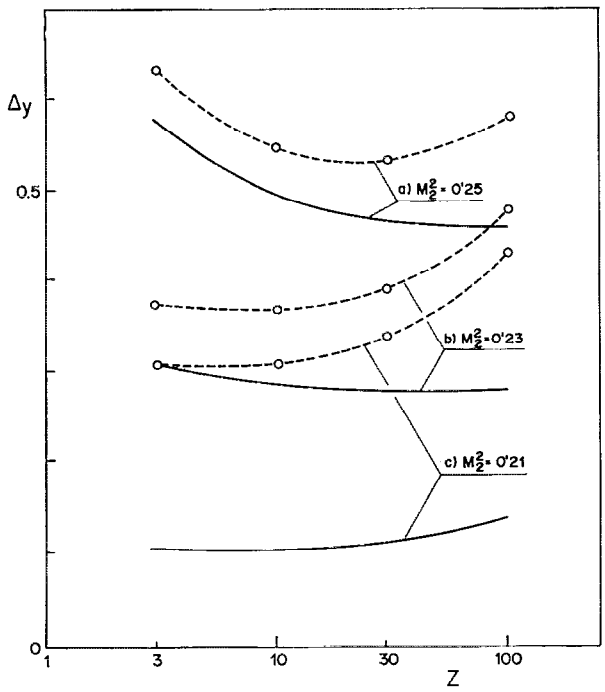

FIG. 3. Dimensionless thickness Δy of the preheating region with local (continuous curves) and nonlocal (dashed curves) electron heat flux for Mach numbers M_1=(a) 3.6, (b) 4.6, and (c) 8.

$$l \equiv H_I \Delta y = \Delta y \frac{9\sqrt{3}}{10\sqrt{10\pi}} \sqrt{\frac{m_i}{m_e}} \frac{\gamma_0(Z)}{(1+Z)^{3/2}} \frac{(kT_2)^2}{e^4 n_2 \ln \Lambda_{ei}}, \quad (24)$$

where, for comparison sake, we use the local dimensionless thickness Δy given in Fig. 3, which is a function of M_1 and, in a lesser degree, of Z. A representative thermal mean-free path for electron scattering is given by[1]

$$\lambda_T \equiv \frac{8}{3} \sqrt{\frac{2kT_e}{\pi m_e}} \frac{Z_*}{11/3+Z_*} \tau_{ei}, \quad (25)$$

where τ_{ei} is defined in (6), and we shall evaluate it at downstream conditions. Comparing Eqs. (24) and (25) one obtains

$$\frac{\lambda_T}{l} = \frac{0.038}{\Delta y} \frac{(1+Z)^{3/2}}{\gamma_0(Z)(11/3+Z)Z^{1/2}}, \quad (26)$$

where we have taken $\sqrt{m_i/m_e Z} \simeq 60$ (fully ionized plasma) and $Z_*=Z$. Table I shows λ_T/l for some values of M_1 and Z. Since $\lambda_T/l < O(1)$ for all values of M_1 and Z, the present results are within the validity range of the nonlocal formulation, which just extends it to the original expectations of the collisional kinetic theory.[1] However, even for very strong shocks, the Knudsen number is relatively small, thus explaining the fact that the global modifications in the shock structure introduced by the nonlocal formulation are less significant than one would expect for strong shocks. These modifications are, nevertheless, locally important (in the foot of the preheating region, see Fig. 2) for Knudsen number even lower than 10^{-2}, as proved by the high values of the relative difference $|\Delta_{nl} y - \Delta y|/\Delta y$ between nonlocal $\Delta_{nl} y$ and local Δy thicknesses, also shown in Table I. This failure of the local heat flux for so small Kundsen numbers is a well-known fact which makes it necessary the use of nonlocal formulations for some important problems of plasma physics (e.g., inertial confinement fusion).[2,6] Here, we give, quantitatively, the errors of the local theory, in relation to the nonlocal one, as a function of the Knudsen number in a physical problem of interest.

TABLE I. Knudsen number λ_T/l, as defined by Eq. (26), for some values of Z and M_1. The relative difference $|\Delta_{nl} y - \Delta y|/\Delta y$ between nonlocal $\Delta_{nl} y$ and local Δy preheating thickness (taken from Fig. 3) is shown in parentheses.

Z \ M_1	3.6	4.8	8
3	0.0086(0.10)	0.017(0.21)	0.047(1.86)
30	0.0066(0.14)	0.011(0.53)	0.028(1.96)
100	0.0065(0.25)	0.011(0.72)	0.023(2.05)

A final comment should be made on the validity of the local transport for the ions used in this work. As the Mach number increases, the ionic gradients become steeper, and, obviously, the classical expressions for the ionic viscosity and thermal conduction are no longer valid inside the ionic shock front.[7] However, this does not affect to the main scope of this work, which is to quantify the effect of the nonlocal electron heat transport on the shock structure, because these nonlocal effects are only important, as we have seen, in the initial part of the electronic preheating region (see Fig. 2), where the velocity and ionic temperatures change smoothly even for very strong shocks, and the classical transport expressions are valid. Thus, though a kinetic formulation should be used to describe the ionic magnitudes for strong shocks, which also will change the electron temperature, these changes are outside the region, where the nonlocal electron heat flux differs from the local one.

ACKNOWLEDGMENT

This work has been supported by the Comisión Interministerial de Ciencia y Tecnología of Spain (PB88-0162).

APPENDIX: LOCAL SHOCK STRUCTURE FOR ANY Z

We describe here, briefly, the solution of Eqs. (2)–(5) in the local limit, generalizing the results of Jaffrin and Probstein[3] for any Z. For the outer regions (regions I and III) one has the following differential equations for η and θ_e [from Eqs. (17)–(19) in the local limit]:

$$\theta_e^{5/2} \frac{d\theta_e}{dy} = 4M_2^3(\eta-1)(\eta_1-\eta), \quad (A1)$$

$$\left[\frac{1+Z}{3}\left(\frac{5}{3}M_2^2(5-8\eta)+5\right)-\frac{2}{3}Z\frac{\theta_e}{\eta}\right]\frac{d\eta}{dy} = \frac{4ZM_2^3}{\theta_e^{5/2}}(\eta-1)(\eta_1-\eta)+\frac{\gamma_0(Z)}{M_2^2}\left(\frac{6}{5}\frac{Z}{1+Z}\right)^2\frac{\theta_e-\theta_i}{\eta^2\theta_e^{3/2}}, \quad (A2)$$

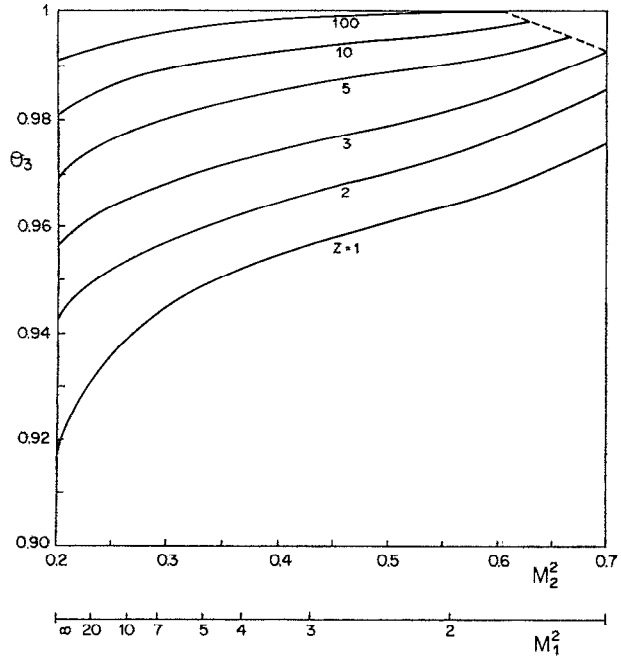

FIG. 4. Electron temperature θ_3 at the ionic shock front as a function of the Mach number for different values of Z.

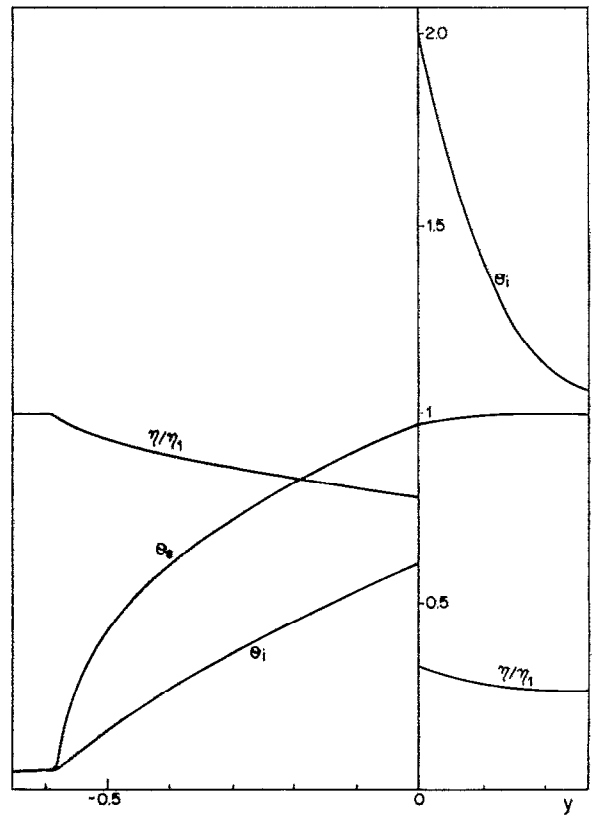

FIG. 5. Shock structure in the local limit ($Z=5$, $M_1=8$).

where θ_i is given by the algebraic equation (17). Linear analysis near the upstream singular point (θ_1,η_1) shows that it is a saddle for any value of $M_2(1/5<M_2^2<1)$. The downstream singular point $(\theta_2,\eta_2)=(1,1)$ is a node for $1\geqslant M_2^2>M^*$ [where M^* is given by (20)], and a saddle point otherwise $(1/5<M_2^2<M^*)$. To obtain the numerical solution of Eqs. (27) and (28) one starts the integration at the upstream point (θ_1,η_1) using the linear local behavior, and reaches the downstream point (1,1) provided that $M_2^2>M^*$; thus, for $M_2^2>M^*$ one has a relaxation shock, without inner ionic shock. For $M_2^2<M^*$, the solution leaving point 1 and reaching 2, which now is also a saddle, presents an unphysical electron temperature overshoot, so that a inner layer should appears (region II) where θ_e remains almost constant, and η and θ_i change abruptly. To obtain the end points of this inner layer, $(\theta_{e3},\theta_{i3},\eta_3)$ and $(\theta_{e4},\theta_{i4},\eta_4)$, where $\theta_{e3}=\theta_{e4}\equiv\theta_3$, Eqs. (21) and (22) should be used (these equations are not affected by the *nonlocal* electron heat flux). Neglecting all the gradients in these equations and eliminating constant G, the following relation is obtained for the upstream and downstream velocities η_3 and η_4 as a function of θ_3:

$$5\left(\frac{5}{3}M_2^2+1\right)(\eta_3-\eta_4)-\frac{20}{3}M_2^2(\eta_3^2-\eta_4^2)=\frac{2Z}{1+Z}\theta_3\ln\frac{\eta_3}{\eta_4}. \tag{A3}$$

On the other hand, one has the functions $\eta_{\rm I}(\theta)$ and $\eta_{\rm III}(\theta)$ resulting from the numerical integration of Eqs. (27) and (28) starting at points 1 and 2, respectively. The value θ_3 is that satisfying (29) if one identifies $\eta_{\rm I}(\theta)=\eta_3(\theta_3)$ and $\eta_{\rm III}(\theta)=\eta_4(\theta_3)$. Figure 4 shows θ_3 as a function of $M_2^2(<M^*)$ for some values of Z. It should be noticed that θ_3 is always very close to unity, so that the electron temperature undergoes almost all its change in region I. Once θ_3, η_3, and η_4 are known, θ_{i3} and θ_{i4} are given by Eqs. (21) and (22) with all the gradients dropped. At the scale length of the outer shock ($H_{\rm I}\sim\lambda_{i2}\sqrt{m_i/m_e}$), the shock structure is given by the numerical solution of Eqs. (27) and (28) from (θ_1,η_1) to (θ_3,η_3) (region I), and from (θ_2,η_2) to (θ_3,η_4) (region III), in addition to a discontinuity given by the jumps $\eta_3-\eta_4>0$ and $\theta_{i4}-\theta_{i3}>0$ (region II) situated at the electron temperature θ_3 (see Fig. 5). The detailed structure of the inner ionic shock may be obtained from Eqs. (21) and (22) once the end points 3 and 4 have been found. It can be shown[3] that point 4 is a saddle, while point 3 is a node, so that the numerical integration of Eqs. (21) and (22) is carried out starting from 4 toward 3.

[1] J. R. Sanmartín, J. Ramírez, R. Fernández-Feria, and F. Minotti, Phys. Fluids B **4**, 3579 (1992).

[2] J. F. Luciani, P. Mora, and J. Virmont, Phys. Rev. Lett. **51**, 1664 (1983); J. A. Albritton, E. A. Williams, I. B. Bernstein, and K. P. Swartz, Phys. Rev. Lett. **57**, 1887 (1986); J. R. Sanmartín, J. Ramírez, and R. Fernández-Feria, Phys. Fluids B **2**, 2519 (1990).

[3] M. Y. Jaffrin and R. F. Probstein, Phys. Fluids **7**, 1658 (1964).

[4] S. I. Braginskii, in *Review of Plasma Physics*, edited by M. A. Leontovich (Consultants Bureau, New York, 1965), Vol. 1, pp. 205–311.

[5] Ya. B. Zel'dovich and Yu. P. Raizer, *Physics of Shock Waves and High-Temperature Hydrodynamic Phenomena* (Academic, New York, 1967), Vol. II, Chap. VIII.

[6] J. Ramírez, and J. R. Sanmartín, *Selfsimilar Expansion of Laser Plasmas with Nonlocal Heat Flux*," Laser Part. Beams (in press).

[7] M. Casanova, O. Larroche, and J. P. Matte, Phys. Rev. Lett. **67**, 2143 (1991).